J Nanostruct 11(3): 609-617, Summer 2021

RESEARCH PAPER

Dye-sensitized Solar Cells Based on Silicon Dioxide Nanoparticles Photochemically Synthesized: A Comparative Study in the Concentration of the Dye-sensitized

Ahmed Mahdi Rheima

University of Wasit, College of Science, Department of Chemistry, kut. Iraq

ARTICLE INFO

Article History:
Received 04 March 2021
Accepted 30 May 2021
Published 01 July 2021

Keywords:
Dye-sensitized solar cell
Photolysis method
Rhodamine 6G
Silicon dioxide nanoparticles

ABSTRACT

Green energy is often derived from renewable energy technologies such as solar, wind, geothermal, biomass, and hydroelectric power as a source of energy. Every one of those technologies generates energy differently, whether it's by harnessing the sun's energy through solar panels, wind turbines, or the flow of water. In recent years, nanomaterials have been used in solar cells due to their high efficiency. Our study reported a new method (photolysis) to fabricate silicon dioxide (SiO_2) nanoparticles. Various techniques investigated the synthesized sample. A transmitted electron microscope (TEM) was used to determine the particle size of nano-SiO_2 and was found to be 20.7 nm. The amorphous structure of SiO_2 nanoparticles synthesized was diagnoses via x-ray diffraction (XRD). The energy band gap is estimated to be 3.61 eV in Uv-visible spectroscopy to evaluate the nano-sample's optical properties. Eventually, SiO_2 nanoparticles were applied as a photoanode to assembled dye-sensitized solar cells (DSSC). Photo-current short-circuits, photovoltaic open-circuit, and DSSC power conversion output was evaluated using an I – V measurement system. The effects of the concentration of Rhodamine 6G dye-sensitized on DSSC power conversion performance have also been studied. The cell power conversion efficiency with increased dye concentrations was mainly increased, with maximum efficiency of 2% at 20 mm of dye concentration. Finally, it can be reported that silicon oxide nanoparticles can be used as anode electrodes in dye-sensitized solar cells, as they are highly effective.

How to cite this article
Rheima A. M , Dorkoosh FA. Dye-sensitized Solar Cells Based on Silicon Dioxide Nanoparticles Photochemically Synthesized: A Comparative Study in the Concentration of the Dye-sensitized. J Nanostruct, 2021; 11(2):609-617. DOI: 110.22052/JNS.2021.03.018

INTRODUCTION

Nanomaterials are quickly spread across all essential science and technology sectors, including electronics, aerospace, defence, medicine, and dentistry [1-4]. It means the design, synthesis, characterization, and use of nanometer-scale materials and tools [4,5]. Physical, chemical, and biological properties in nanoscales differ from individual bulk atoms and molecules [6-8]. This allows creating new groups of advanced materials and compounds that fulfil high technology applications requirements [9-12]. Because of its broad applications in electronic equipment, insulators catalyzes or pharmaceuticals; The scientific community has given silica nanoparticles intense study [14]. Nanoparticles from SiO_2 Amorphous are used to produce electronic

* Corresponding Author Email: arahema@uowasit.edu.iq

substrates, film substrates, insulators for electrical purposes, insulators, and humidity sensors [15-17]. For each of these products, silica particles play a different function. Some products rely on their quality on silica particles' amount and scale [18]. Small-scale silica particles with a high purity like high-tech are essential. Industries such as biotechnology and photonics are highly demanding of this sort of material. The optical properties of silica nanoparticles can be observed for surface defects consistent with large surface/volume ratios[19,20].

Different techniques such as processing microemulsion, chemical vapour deposition (CVD), hydrothermal techniques, combustion synthesis, plasma-synthesis, sol-gel techniques, etc., have been applied to the synthesis of SiO_2 nanoparticles [21-24]. Regardless of the synthesis process, the main emphasis was on particle size, morphology regulation, and particle surface [25]. Our method (photolysis method) is considered new in the synthesis of SiO_2 nanoparticles, whereby we can control the particle size without any aggregation [26,27]. In a solar cell application, Improved photon absorption and load carriers' production are the essential requirements in the form of DSSC. Therefore, because of their fundamental properties that can improve solar cells' converting power, Nanomaterials are used in photovoltaic (PV) technology. They are found promising for visible spectral area light harvesting because of the improved electron mobility resulting from the generation of fast charging carrier [28-30]. Due to their unique physical and chemical properties, SiO_2 nanoparticles have been used in solar cell applications. This material also has excellent electrical and optical properties [31].

Consequently, sensors, piezoelectric devices, fuel cells, anti-reflection coating, catalysts were used [32-34]. A dye-sensitized solar cell (DSSC) is a part of the 3rd solar cell generation. DSSC does not require high pure content and relatively low manufacturing costs [35]. It involves four main components impacting cell activity: photoanode, a counter electrode, Dye-sensitized, and electrolytes [36]. In this paper, silicon dioxide nanoparticles were synthesized by a new method (photolysis method) and usage as a photo-anode to Fabrication Dye-sensitized solar cell (DSSC).

MATERIALS AND METHODS

All materials were purchased and used as received from Sigma-Aldrich. Throughout the preparation and purification steps. Tetraethylorthosilicate (purity 98%), acetic acid (purity 99.8%), absolute ethanol (EtOH purity 99.9%), Rhodamine 6G dye, and urea (purity 99.9%) have been used in this work.

Synthesis of silicon dioxide (SiO_2) Nanoparticles

UV irradiation was used as a source to synthesis SiO_2 NPs by mixing 20 ml of Tetraethylorthosilicate with 60 ml of acetic acid\ water (1:5). The mixture was stirred for 5 minutes; then, 20 ml, 0.2 M of urea was added slowly to the above solution. The UV source is a mercury lamp (λ = 365 nm) operating at 125 W. The irradiation lamp was immersed inside the chemical reaction, as shown in Fig. 1. An ice bath cooled the system to control the temperature. After 30 minutes, a gel of white colour was formed, the gel was separated and washed several times by absolute ethanol, then dried at 100 °C and calcinated in an oven at 600 °C for 3 hours. A white powder of silicon dioxide

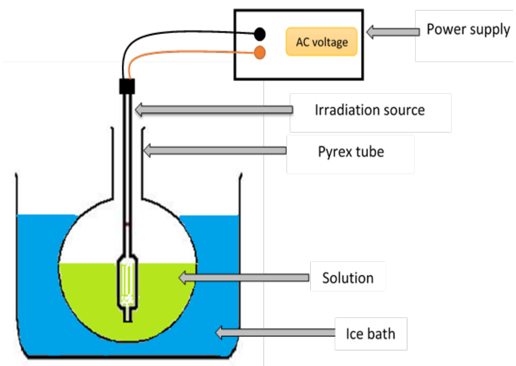

Fig. 1. Synthesis of silicon dioxide nanoparticles using the UV-irradiation method.

nanoparticles was obtained.

Fabrication of silicon dioxide-based on dye-sensitized solar cell

SiO_2 nanoparticles were coated onto the indium-doped tin oxide (ITO) glass, resistance 8 ohm, and transmission 83%. ITO glass (2 x 2 x 1 mm) was washed with ethanol and de-ionized water several times with an ultrasonic bath for impurity clearance and dry using an air blower. SiO_2 nanoparticles were coating accordingly; a colloidal solution of SiO_2 nanoparticles had prepared by mixing 500 mg of the nano-powder with 20 ml of ethanol. The photoanode was done utilizing a dripper to cover the ITO-glass's conductive face with a colloidal solution, then annealed at 250°C for 60 minutes in the air.

The annealed film had immersed overnight at room temperature in the different concentrations (5, 10, 15, 20 mM) of Rhodamine 6G dye ($C_{28}H_{31}ClN_2O_3$) using de-ionized water as a solvent [37]. Graphene -silver nanocomposite was prepared by hummer's modified method [38]. Then, coated on the conductive side of ITO glass by immersed it overnight in a colloidal solution of 200 mg graphene -silver nanocomposite with 20 ml of ethanol and used as a counter electrode. The dye-absorbed SiO_2 nanoparticles coated ITO glass was clipped with a Graphene -silver nanocomposite (G-Ag) coated ITO glass (counter electrode) to make a sandwich-type DSSC design. Finally, the liquid electrolyte (I^- /I^{-3}) solution was immersed in the system through the electrode counter gap. The Fabrication of silicon dioxide-based on the dye-sensitized solar cell is shown in Fig. 2.

Characterization

X-ray diffraction of SiO_2 nanoparticles was examined using (XRD-6000) which was operated at 30 mA and 40 kV to generate radiation at a wavelength of 1.5406 Å. JEOL JEM-2100 TEM measurement was used to study nanoparticles' size and morphology. A drop of suspended nanoparticles was placed on the carbon-coated TEM grid for analysis. Shimadzu UV-Vis 160 V spectrometer measured the absorbance of SiO_2 nanoparticles.

RESULT AND DISCUSSION

Structure of SiO_2 nanoparticles

As a part of this investigation, the diffraction angle 2θ of XRD analysis spanning the 5−80 degree range were carried out to test the obtained SiO_2 nanoparticles, as shown in Fig. 3. The powder diffraction pattern indicates a typical broad peak at 2θ = 22°, which reveals the amorphous existence of silica [39]. The XRD pattern also shows that no

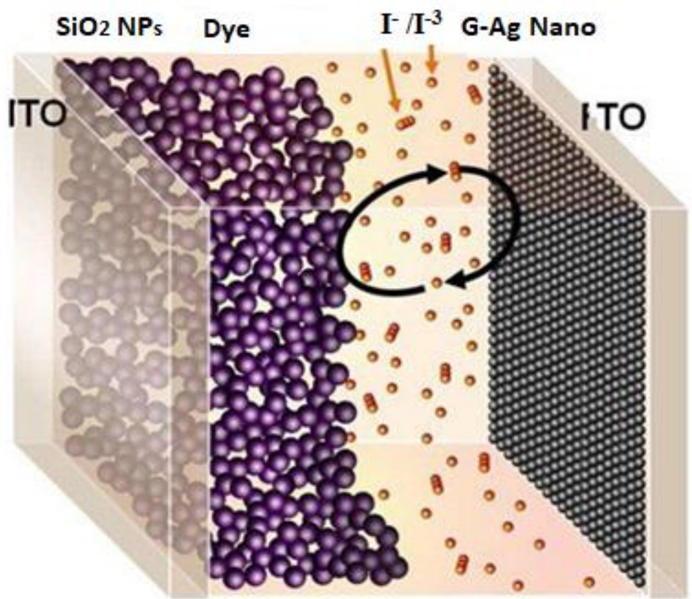

Fig. 2. Graphical structure of SiO_2 nanoparticles based DSSC

ordered crystalline structure is present.

The small size and incomplete internal structure of synthesized powders may be responsible for this high XRD reflecting point. There is no other high impurity reflecting silica nanoparticles' pureness. The XRD results can be used to determine the crystal size of SiO_2 nanoparticles. In this work, the average size (D) of SiO_2 nanoparticles was calculated using the Debye-Scherrer equation [40-44]:

$$D = K\lambda / \beta\cos \quad (1)$$

Where k denotes Scherrer constant that equals 0. 9, λ is the wavelength of the Cu-Kα radiation, β corresponds to line broadening in radians (the full width at half maximum, FWHM) and θ is the Bragg angle derived from the 2θ value corresponding to

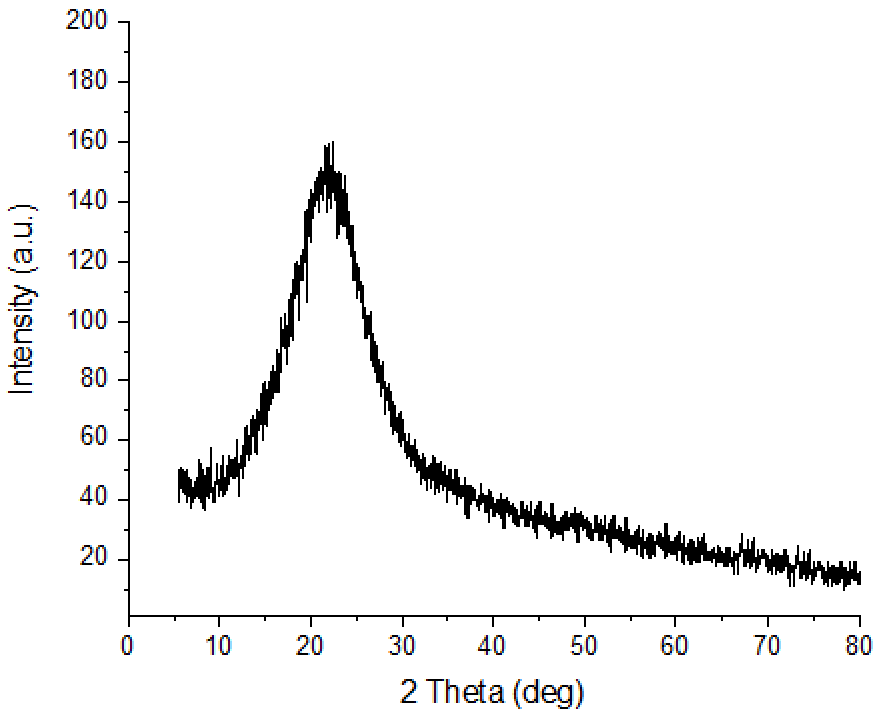

Fig. 3. Synthesis of silicon dioxide nanoparticles using the UV-irradiation method.

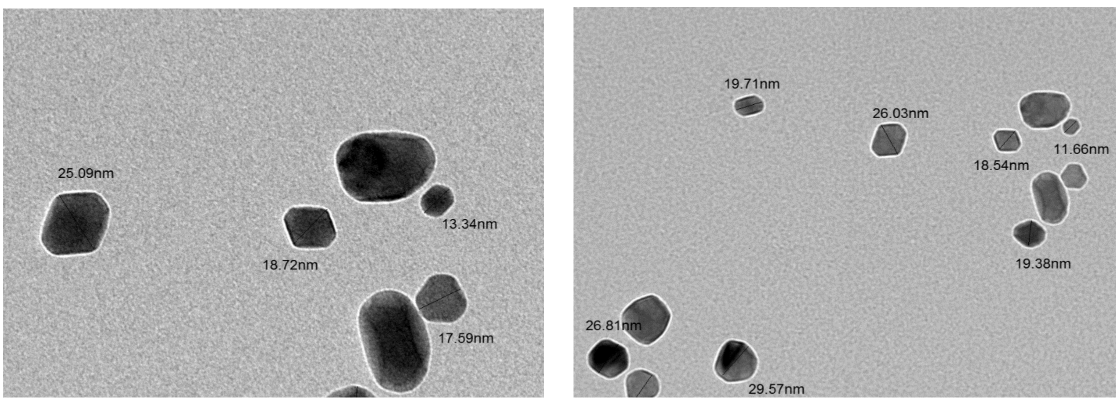

Fig. 4. TEM images of SiO_2 nanoparticles at two different scales (50 and 100 nm).

the maximum peak-intensity in the XRD pattern. The SiO_2 nanoparticles diameter obtained using Eq. (1) was 11.79 nm. Thus, our experiment's UV source was proved to produce SiO_2 nanoparticles.

Transmission electron microscopy (TEM)

In SiO_2 nanoparticle characterization, TEM was chosen because it produces a higher resolution and greater precision in particle size in contrast to others, including electron microscopy scanning. Fig. 4. shows high-scale TEM images on two different scales (50 and 100 nm) of SiO_2 nanoparticles. Subsequent TEM characterization studies have verified the actual scale, shape, and morphology of nanoparticles. Furthermore, the images show that the SiO_2 nanoparticles are quasi-spherical without aggregation. Based on these experiments, the average size of the nanoparticle 20.7 nm was achieved after the average XRD measurement of nanoparticle size. That has been consistent.

Optical properties of SiO_2 nanoparticles

The optical band gap of SiO_2 nanoparticles was tested using UV-vis spectroscopy in the range of 200–800 nm. Dispersed into de-ionized water by sonication for 5 min, the synthesized SiO_2 nanoparticles obtained a uniform solution. Fig. 5 (a) reveals a SiO_2 nanoparticles UV-visible spectrum. The spectrum shows a high absorption peak at 317 nm due to SiO_2 nanoparticles surface Plasmon absorption. The absorption edge of SiO_2 nanoparticles was at 363 nm.

The optical band gap of SiO_2 nanoparticles was calculated by Tauc equation [45]:

$$(\alpha h\nu)^2 = A(h\nu - E_g) \tag{2}$$

where E_g = energy of the optical bandgap, α = absorbance, h = planks constant, υ = frequency of incident radiation, A = constant called the band tailing parameter.

Plotting $(\alpha h\nu)^2$ versus Eg based on the spectral response gives the extrapolated intercept, which corresponds to the bandgap energy values, as shown in Fig. 5 (b). The optical band gap energy of the SiO_2 nanoparticles is measured to be 3.61 eV.

photovoltaic properties of DSSC based on SiO_2 nanoparticles

The photovoltaic parameters of the dye-sensitized solar cell (DSSC) with different dye concentrations made by SiO_2 nanoparticles are shown in Fig. 6. The results of these performances are summarized in Table 1. A solar simulator includes the DSSC, illuminated by a 100 mW / cm^2 halogen lamp. The power conversion efficiency of DSSC was calculated by [40,46,47]:

$$\eta = P_{max} / P_{in} = V_{oc}.J_{sc}.FF / P_{in} * 100\ \% \tag{3}$$

where , and Represent the value of open-circuit photovoltage, the value of photo-current of short-circuit density, and incident light power, respectively. The fill factor (FF) is defined by [40]:

$$FF = V_{max}.\, J_{max} / V_{oc}.\, J_{sc} \tag{4}$$

where and Represent the voltage and the current density at the maximum output power.

The DSSC values are calculated in Table 1. It was critical for the SiO_2-based DSSC parameters

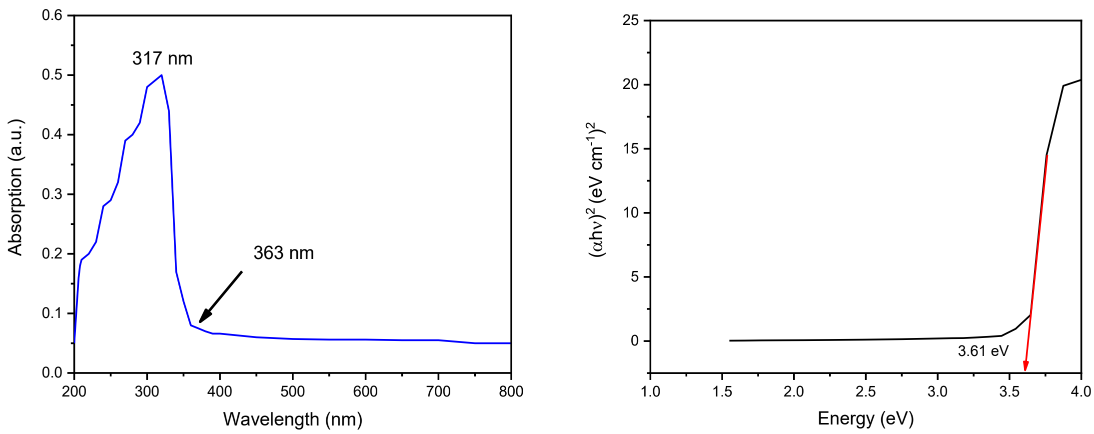

Fig. 5. (a) UV-visible spectra of synthesized SiO_2 nanoparticles (b) The Plot of versus the energy of SiO_2 nanoparticles bandgap.

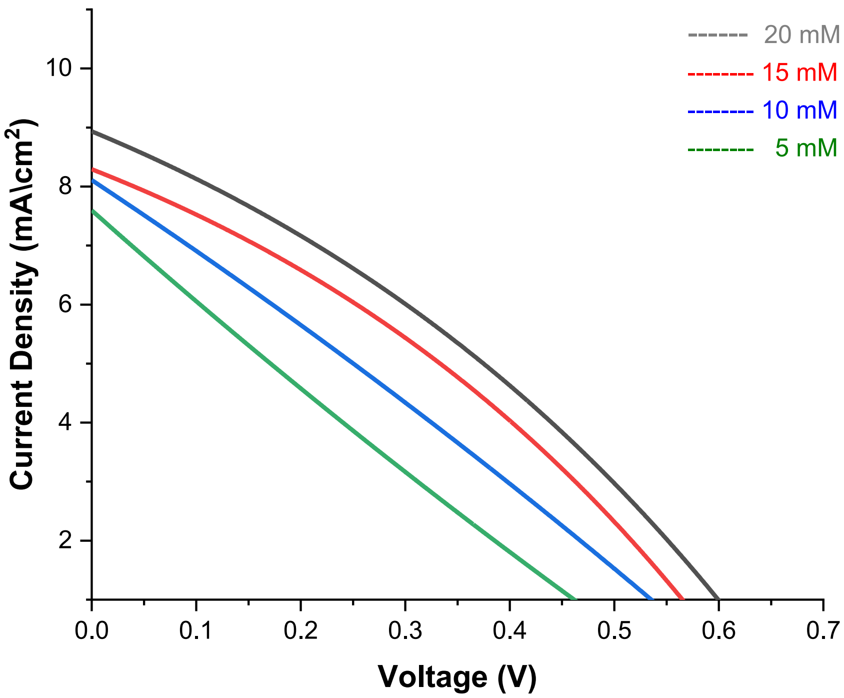

Fig. 6. J-V curve of SiO_2 nanoparticles-based DSSC by different concentrations

because of the concentration sensitizing dye and small particles of synthesized SiO_2 nanoparticles. The cell power conversion efficiency was increased with increased dye concentrations. The increased absorption may also explain the dye molecules' high efficiency on the SiO_2 surface. Therefore, SiO_2 nanoparticles are promising to be used in potential photovoltaics as the process is easy, and the materials can quickly be prepared. There was a relatively low current density rating. The photo-current is the most critical parameter for calculating the overall system efficiency limit. The parent materials act differently because of their large surface area and surface energy when their particle size approaches the nano level. The synthesized SiO_2 nanoparticles have an average particle size of approximately 20.7 nm. We can, therefore, expect substantial phytochemicals. A relatively small photo-current may be powered by different factors, such as small roughness factor, ow injection efficiency, photoanode reflection or dispersion, and charging performance.

Consequently, additional electron densities at higher light intensity were transferred to SiO_2. Table 1 shows that the values η and Jsc increase as the light density applied increases. The increase in control generation is due to the rise in light intensity. The highest short circuit current and high open-circuit voltage were shown on our DSSC, with a 20 mM photosensor concentration. Due to the SiO_2 nanoparticle molecular structure (favorable with electron/hole pair separation). The DSSC mechanism can be discussed, To enter the excited state, light passes through a transparent electrode and is absorbed by Rhodamine 6G dye. The excited electrons would then be pumped into

Table 1. The parameters of SiO_2 nanoparticles- based DSSC

The concentration of Rhodamine 6G dye sensitizer [mM]	V_{oc} (V)	J_{sc} (mA\cm²)	V_{max} (V)	J_{max} (mA\cm²)	P_{max} (mW\cm²)	FF	η %
5	0.51	8.11	0.25	4.09	1.0225	0.247	1.02 %
10	0.56	8.51	0.29	4.43	1.2847	0.269	1.28 %
15	0.59	9.02	0.34	5.10	1.734	0.326	1.73 %
20	0.61	9.40	0.35	5.72	2.002	0.349	% 2

the semiconductor SiO_2 Nanoparticles conduction band and transferred to an external circuit. To complete a loop, the oxidized dye would be reduced by a redox pair in the electrolyte, which a counter electrode would then reduce with external circuit electrons. In comparing the SiO_2 nanoparticles-based DSSC with previously reported DSSC [48-52], the obtained DSSC in this study can be regarded as an active photoanode with a counter electrode to fabrication SiO_2 nanoparticles-based DSSC Which gives high conversion efficiency as a result of the preference of silicon oxide in dye solar cells.

CONCLUSIONS

The dye-sensitized solar cell (DSSCs(based on SiO_2 nanoparticles was provided in this report. In particular, the nano-size SiO_2 powders have been synthesized by the photolysis method; This method has the advantage of giving us a small size of particles without any aggregation. TEM, XRD, and UV-visible have characterized the Synthesized nano-powders. 20.7 nm is the size of the average particles we got from the TEM measurement. The energy band gap was 3.61 ev. The effects on the DSSC power conversion efficiency have also been studied in the concentration of Dye-sensitized Rhodamine 6G. Cell power conversion efficiency was mainly increased at an increased dye concentration. The maximum efficiency was 2.00% at a concentration of 20 mM Rhodamine 6G dye under an input light intensity of 100 mW\cm^2.

CONFLICT OF INTEREST

The authors declare that there are no conflicts of interest regarding the publication of this manuscript.

REFERENCES

1. Karimi-Maleh H, Yola ML, Atar N, Orooji Y, Karimi F, Kumar PS, Rouhi J, Baghayeri M. A novel detection method for organophosphorus insecticide fenamiphos: Molecularly imprinted electrochemical sensor based on core-shell Co_3O_4@ MOF-74 nanocomposite. Journal of colloid and interface science. 2021;592:174-185.
2. Karimi-Maleh H, Ranjbari S, Tanhaei B, Ayati A, Orooji Y, Alizadeh M, Karimi F, Salmanpour S, Rouhi J, Sillanpää M, Sen F. Novel 1-butyl-3-methylimidazolium bromide impregnated chitosan hydrogel beads nanostructure as an efficient nanobio-adsorbent for cationic dye removal: Kinetic study. Environmental research. 2021;195:110809.
3. Nwofe PA, Agbo PE, Ozibo CO. COMPOSITIONAL AND OPTICAL ANALYSIS OF CHEMICALLY DEPOSITED ZINC-DOPED ANTIMONY SULPHIDE THIN FILMS. Chalcogenide Letters. 2016;13(10).
4. Nwofe PA. Study of Composition and Optical Properties of Chemically Deposited Pd-xSb_2S_3 Thin Films. Journal of Nanostructures. 2017;7(3):236-245.
5. Hussain DH, Rheima AM, Jaber SH, Kadhim MM. Cadmium ions pollution treatments in aqueous solution using electrochemically synthesized gamma aluminum oxide nanoparticles with DFT study. Egyptian Journal of Chemistry. 2020;63(2):417-424.
6. Ali AA, Al-Hassani RM, Hussain DH, Rheima AM, Abd AN, Meteab HS. Fabrication of Solar Cells Using Novel Micro- and Nano-Complexes of Triazole Schiff Base Derivatives. Journal of Southwest Jiaotong University. 2019;54(6).
7. Karimi-Maleh H, Alizadeh M, Orooji Y, Karimi F, Baghayeri M, Rouhi J, Tajik S, Beitollahi H, Agarwal S, Gupta VK, Rajendran S. Guanine-based DNA biosensor amplified with Pt/SWCNTs nanocomposite as analytical tool for nanomolar determination of daunorubicin as an anticancer drug: a docking/experimental investigation. Industrial & Engineering Chemistry Research. 2021;60(2):816-823.
8. Karimi-Maleh H, Kumar BG, Rajendran S, Qin J, Vadivel S, Durgalakshmi D, Gracia F, Soto-Moscoso M, Orooji Y, Karimi F. Tuning of metal oxides photocatalytic performance using Ag nanoparticles integration. Journal of Molecular Liquids. 2020;314:113588.
9. Karimi-Maleh H, Cellat K, Arıkan K, Savk A, Karimi F, Şen F. Palladium–Nickel nanoparticles decorated on Functionalized-MWCNT for high precision non-enzymatic glucose sensing. Materials Chemistry and Physics. 2020;250:123042.
10. Karimi-Maleh H, Shafieizadeh M, Taher MA, Opoku F, Kiarii EM, Govender PP, Ranjbari S, Rezapour M, Orooji Y. The role of magnetite/graphene oxide nano-composite as a high-efficiency adsorbent for removal of phenazopyridine residues from water samples, an experimental/theoretical investigation. Journal of Molecular Liquids. 2020;298:112040.
11. Ismail AH, Al-Bairmani HK, Abbas ZS, Rheima AM. Synthesis, Characterization, Spectroscopic and Biological Studies of Zn(II), Mn(II) and Fe(II) Theophylline Complexes in Nanoscale. Nano Biomed. Eng. 2020;12(3).
12. Ismail AH, Al-Bairmani HK, Abbas ZS, Rheima AM. Nano-synthesis, spectroscopic characterisation and antibacterial activity of some metal complexes derived from Theophylline. Egyptian Journal of Chemistry. 2020.
13. Rheima AM, Mohammed MA, Jaber SH, Hasan MH. Inhibition effect of silver-calcium nanocomposite on alanine transaminase enzyme activity in human serum of Iraqi patients with chronic liver disease. Drug Invention Today. 2019;12(11):2818-2821.
14. Rheima AM, Mohammed MA, Jaber SH, Hameed SA. Adsorption of selenium (Se^{4+}) ions pollution by pure rutile titanium dioxide nanosheets electrochemically synthesized. Desalination and Water Treatment. 194 (2020) 187–193.
15. Ali AA, Al-Hassani RM, Hussain DH, Rheima AM, Meteab HS. Synthesis, spectroscopic, characterization, pharmacological evaluation, and cytotoxicity assays of novel nano and micro scale of copper (II) complexes against human breast cancer cells. Drug Invention Today. 2020;14(1).
16. Ismail AH, Al-Bairmani HK, Abbas ZS, Rheima AM. Nanoscale Synthesis of Metal (II) Theophylline Complexes and Assessment of Their Biological Activity. Nano Biomed. Eng. 2020;12(2):139-147.
17. Ismail AH, Al-Bairmani HK, Abbas ZS, Rheima AM. Synthesis, characterization, spectroscopic, and biological activity

studies of Nano scale Zn(II), Mn (II) and Fe (II) theophylline complexes. Journal of Xi'an University of Architecture & Technology. 2020; XII (II): 2775-2789.

18. Jabber SH, Hussain DH, Rheima AM, Faraj M. Comparing study of CuO synthesized by biological and electrochemical methods for biological activity. Al-Mustansiriyah Journal of Science. 2019;30(1):94-98.
19. Sprenger S. Epoxy resin composites with surface-modified silicon dioxide nanoparticles: A review. Journal of Applied Polymer Science. 2013;130(3):1421-1428.
20. Kholodnaya G, Ponomarev D, Sazonov R, Remnev G. Characteristics of pulsed plasma-chemical synthesis of silicon dioxide nanoparticles. Radiation Physics and Chemistry. 2014;103:114-118.
21. Leonard KC, Genthe JR, Sanfilippo JL, Zeltner WA, Anderson MA. Synthesis and characterization of asymmetric electrochemical capacitive deionization materials using nanoporous silicon dioxide and magnesium doped aluminum oxide. Electrochimica Acta. 2009;54(22):5286-5291.
22. Rahman IA, Padavettan V. Synthesis of silica nanoparticles by sol-gel: size-dependent properties, surface modification, and applications in silica-polymer nanocomposites—a review. Journal of Nanomaterials. 2012;2012.
23. Osman NS, Sapawe N. Waste Material As an Alternative Source of Silica Precursor in Silica Nanoparticle Synthesis–A Review. Materials Today: Proceedings. 2019;19:1267-1272.
24. Rubio L, Pyrgiotakis G, Beltran-Huarac J, Zhang Y, Gaurav J, Deloid G, Spyrogianni A, Sarosiek KA, Bello D, Demokritou P. Safer-by-design flame-sprayed silicon dioxide nanoparticles: the role of silanol content on ROS generation, surface activity and cytotoxicity. Particle and fibre toxicology. 2019;16(1):40.
25. Mai BD, Nguyen HT, Nguyen TK, Ta DH, Luu TN. Effects of composition ratio on structure and phase transition of ferroelectric nanocomposites from silicon dioxide nanoparticles and triglycine sulfate. Phase Transitions. 2019;92(6):563-570.
26. Gunday ST, Cevik E, Yusuf A, Bozkurt A. Synthesis, characterization and supercapacitor application of ionic liquid incorporated nanocomposites based on SPSU/Silicon dioxide. Journal of Physics and Chemistry of Solids. 2020;137:109209.
27. Li L, Wang W, Tang J, Wang Y, Liu J, Huang L, Wang Y, Guo F, Wang J, Shen W, Belfiore LA. Classification, synthesis, and application of luminescent silica nanoparticles: a review. Nanoscale research letters. 2019 Dec 1;14(1):190.
28. Jeelani PG, Mulay P, Venkat R, Ramalingam C. Multifaceted application of silica nanoparticles. A review. Silicon. 2020;12(6):1337-1354.
29. Farjadian F, Roointan A, Mohammadi-Samani S, Hosseini M. Mesoporous silica nanoparticles: synthesis, pharmaceutical applications, biodistribution, and biosafety assessment. Chemical Engineering Journal. 2019 Mar 1;359:684-705.
30. Osman NS, Sapawe N. Waste Material As an Alternative Source of Silica Precursor in Silica Nanoparticle Synthesis–A Review. Materials Today: Proceedings. 2019;19:1267-1272.
31. Lin JF, Li J, Gopal A, Munshi T, Chu YW, Wang JX, Liu TT, Shi B, Chen X, Yan L. Synthesis of photo-excited Chlorin e6 conjugated silica nanoparticles for enhanced anti-bacterial efficiency to overcome methicillin-resistant Staphylococcus aureus. Chemical Communications. 2019;55(18):2656-2659.
32. Rheima AM, Mohammed MA, Jaber SH, Hameed SA. Synthesis of silver nanoparticles using the UV-irradiation technique in an antibacterial application. Journal of Southwest Jiaotong University. 2019;54(5).
33. Mohammed MA, Rheima AM, Jaber SH, Hameed SA. The removal of zinc ions from their aqueous solutions by Cr_2O_3 nanoparticles synthesized via the UV-irradiation method. Egyptian Journal of Chemistry. 2020;63(2):425-431.
34. Kadhum, H.A., Salih, W.M. & Rheima, A.M. Improved PSi/c-Si and Ga/PSi/c-Si nanostructures dependent solar cell efficiency. Appl. Phys. A 126, 802 (2020).
35. Siddiqui H, Parra MR, Pandey P, Qureshi MS, Haque FZ. Utility of copper oxide nanoparticles (CuO-NPs) as efficient electron donor material in bulk-heterojunction solar cells with enhanced power conversion efficiency. Journal of Science: Advanced Materials and Devices. 2020.
36. Vasanth A, Powar NS, Krishnan D, Nair SV, Shanmugam M. Electrophoretic Graphene Oxide Surface Passivation on Titanium Dioxide for Dye Sensitized Solar Cell Application. Journal of Science: Advanced Materials and Devices. 2020.
37. Cardoso BN, Kohlrausch EC, Laranjo MT, Benvenutti EV, Balzaretti NM, Arenas LT, Santos MJ, Costa TM. Tuning anatase-rutile phase transition temperature: TiO2/SiO2 nanoparticles applied in dye-sensitized solar cells. International Journal of Photoenergy.;2019.
38 Rheima AM, Hussain DH, Almijbilee MM. Graphene-Silver Nanocomposite: Synthesis, and Adsorption Study of Cibacron Blue Dye from Their Aqueous Solution. Journal of Southwest Jiaotong University. 2019;54(6).
39. Dubey RS, Rajesh YB, More MA. Synthesis and characterization of SiO2 nanoparticles via sol-gel method for industrial applications. Materials Today: Proceedings. 2015;2(4-5):3575-3579.
40. Rheima AM, Hussain DH, Abed HJ. Fabrication of a new photo-sensitized solar cell using TiO_2\ZnO Nanocomposite synthesized via a modified sol-gel Technique. InIOP Conference Series: Materials Science and Engineering 2020 (Vol. 928, No. 5, p. 052036). IOP Publishing.
41. RHEIMA AM, Aboud NA, JASIM BE, ISMAIL AH, ABBAS ZS. Synthesis and structural characterization of $ZnTiO_3$ nanoparticles via modification sol-gel prosses for assessment of their antimicrobial activity. International journal of pharmaceutical research. 2021;13(1).
42. Aboud NA, Alkayat WM, Hussain DH, Rheima AM. A comparative study of ZnO, CuO and a binary mixture of $ZnO_{0.5}$-$CuO_{0.5}$ with nano-dye on the efficiency of the dye-sensitized solar cell. InJournal of Physics: Conference Series 2020 (Vol. 1664, No. 1, p. 012094). IOP Publishing.
43. Rheima AM, Mahmood RS, Hussain DH, Abbas ZS. Study the Adsorption Ability of Alizarin Red Dye From Their Aqueous Solution on Synthesized Carbon Nanotubes. Digest Journal of Nanomaterials and Biostructures. 2020;15(4).
44. Rheima A, Anber AA, Shakir A, Salah Hammed A, Hameed S. Novel method to synthesis nickel oxide nanoparticles for antibacterial activity. Iranian Journal of Physics Research. 2020;20(3):51-55.
45. Jubu PR, Yam FK, Igba VM, Beh KP. Tauc-plot scale and extrapolation effect on bandgap estimation from UV–vis–NIR data–a case study of β-Ga_2O_3. Journal of Solid State Chemistry. 2020;290:121576.
46. Hussain DH, Abdulah HI, Rheima AM. Synthesis and Characterization of ɣ-Fe2O3 Nanoparticles Photo Anode by Novel Method for Dye Sensitized Solar Cell. International

Journal of Scientific and Research Publications. 2016;6(10):26-31.
47. Rheima, A.M., D.H. Hussain, and H.I. Abdulah, Silver nanoparticles : Synthesis, Characterization and their used a counter electrodes in novel Dye sensitizer solar cell. IOSR Journal of Applied Chemistry, 2016. 9(10): p. 6–9.
48. Oh K, Kwon O, Son B, Lee DH, Shanmugam S. Nafion-sulfonated silica composite membrane for proton exchange membrane fuel cells under operating low humidity condition. Journal of Membrane Science. 2019;583:103-9.
49. Cardoso BN, Kohlrausch EC, Laranjo MT, Benvenutti EV, Balzaretti NM, Arenas LT, Santos MJ, Costa TM. Tuning anatase-rutile phase transition temperature: TiO_2/SiO_2 nanoparticles applied in dye-sensitized solar cells. International Journal of Photoenergy. 2019;2019.
50. Neshat A, Safdari R. Enhancement in Dye-Sensitized Solar Cells Using Surface Plasmon Resonance Effects from Colloidal Core-Shell Au@ SiO_2 Nanoparticles. ChemistrySelect. 2019;4(17):4995-5001.
51. Jiao S, Sun Z, Wen J, Liu Y, Li F, Miao Q, Wu W, Li L, Zhou Y. Development of Rapid Curing SiO_2 Aerogel Composite-Based Quasi-Solid-State Dye-Sensitized Solar Cells through Screen-Printing Technology. ACS Applied Materials & Interfaces. 2020;12(43):48794-48803.
52. Li M, Yuan N, Tang Y, Pei L, Zhu Y, Liu J, Bai L, Li M. Performance optimization of dye-sensitized solar cells by gradient-ascent architecture of SiO_2@ Au@ TiO_2 microspheres embedded with Au nanoparticles. Journal of materials science & technology. 2019;35(4):604-609.